

## Three New Species of *Tursiocola* (Bacillariophyta) from the Skin of the West Indian Manatee (*Trichechus manatus*)

THOMAS A. FRANKOVICH<sup>1,\*</sup>, MICHAEL J. SULLIVAN<sup>2</sup> & NICOLE I. STACY<sup>3</sup>

<sup>1</sup>Florida International University, Florida Bay Interagency Science Center, 98630 Overseas Highway, Key Largo, FL 33037, USA

<sup>2</sup>130 Martinique Drive, Madison, MS 39110, USA; E-mail: [sullivanmi@gosaints.org](mailto:sullivanmi@gosaints.org)

<sup>3</sup>University of Florida, Large Animal Clinical Sciences, Gainesville, FL 32641, USA; E-mail: [stacyn@ufl.edu](mailto:stacyn@ufl.edu)

\* Corresponding author (E-mail: [frankovich@virginia.edu](mailto:frankovich@virginia.edu))

### Abstract

Three new species of *Tursiocola* are described from the skin of the West Indian manatee bringing the total number of known species in the genus to seven. The range of morphological diversity within the genus is greatly expanded. The number of poroid rows on the copulae is no longer a valid characteristic for the separation of *Tursiocola* from the ceticolous genus *Epiphalaina*. The presence of a butterfly-like structure in the central area of the former is at present the best criterion for separating the 2 genera. The 3 new *Tursiocola* species accounted for nearly 90% of all diatom valves on the manatee skin. No other diatom taxa previously described as new from the skin of cetaceans were present on the manatee.

**Keywords:** biogeographical distribution, epidermal diatoms, Florida, LM, morphology, SEM

### Introduction

Unique epizoid diatom floras have been described from marine mammals (see Tiffany 2011 for review). Cetaceans have been the only marine mammal group from which epizoid diatoms were observed (Bennet 1920, Hart 1935). Subsequent investigators of epidermal diatom assemblages from dead whales and porpoises from whaling stations and stranding events have identified obligate epizoid pennate diatoms comprising several genera including *Plumosigma* Nemoto (1956: 111), *Bennettella* Holmes (1985: 48), *Epipellis* Holmes (1985: 53), *Epiphalaina* Holmes, Nagasawa & Takano (1993a: 4), *Tursiocola* Holmes, Nagasawa & Takano (1993: 5), and *Tripterion* Holmes, Nagasawa & Takano (1993a: 7) (Hustedt 1952; Nemoto 1956; Nemoto *et al.* 1980; Holmes 1985; Holmes *et al.* 1989, 1993a; Denys 1997). Though benthic and planktonic diatoms from the marine littoral have also been observed on cetaceans, an endemic flora generally dominates these communities (Denys 1997).

Of particular interest to the present study are the two closely related genera, *Epiphalaina* and *Tursiocola* (Holmes *et al.* 1993a), created by the transfer of the ceticolous taxa *Stauroneis aleutica* Nemoto (1956: 110) and *S. olympica* Hustedt (1952: 288), respectively. Currently, *Epiphalaina* is comprised of three taxa: *E. aleutica* (Nemoto) Holmes, Nagasawa & Takano (1993a: 5), *E. aleutica* var. *lineata* Denys, (1997: 5) and *E. radiata* Holmes, Nagasawa & Takano (1993b: 128), while *Tursiocola* has four taxa: *T. olympica* (Hustedt) Holmes, Nagasawa & Takano (1993a: 6), *T. omurai* (Nemoto 1956: 110) Denys (1997: 7), *T. staurolineata* Denys (1997: 8), and *T. podocnemicola* Wetzel, Van de Vijver & Ector (2012: 2). The recently described *T. podocnemicola* is the first taxon of these genera to be described from an animal (freshwater turtle) other than cetaceans (Wetzel *et al.* 2012), though an unidentified *Tursiocola* species was reported from sea turtles (Mariska Brady, pers. comm.), and *T. olympica* was reported on the barnacle *Coronula diadema* (Hustedt 1952).

The degree of host specificity of these endemic epizoid diatoms is not yet known due to the scarcity of samples from vertebrate animals other than the cetaceans. Holmes *et al.* (1993b) concluded that host specificity was not present within the cetaceans and speculated that ceticolous taxa may be found on other hosts as well. Studies of epizoid diatoms on other aquatic and marine vertebrate hosts are few in number (Wetzel *et al.* 2012). This current scarcity does not allow any conclusions to be made regarding host specificity of endemic diatom communities within and among other groups of marine and aquatic animals.

Unique and unknown diatoms were recently observed in a veterinary investigation that was conducted to differentiate diatoms from parasite ova and protozoa in cytologic samples from manatees, bottlenose dolphins, and a seahorse (Stacy *et al.* 2014). Scanning electron microscopy (SEM) analyses of some of the unknown taxa from a West Indian manatee (*Trichechus manatus* Linnaeus 1758: 34) revealed similarities to *Epiphialina* and *Tursiocola*. The present study describes three new taxa from the manatee skin and discusses morphological affinities with established taxa. This is the first report of epizoic diatoms on a manatee.

## Materials & Methods

On October 28, 2013 a recently deceased adult female West Indian manatee *Trichechus manatus* (cause of death unknown) was found in the vicinity of Coon Key, Florida Bay, FL, USA (25° 03' 18" N, 80° 44' 10" W) and reported to Everglades National Park rangers. With the assistance of park rangers, feces and a 30 cm<sup>2</sup> piece of dried skin from the belly area, which had already separated from the dead mammal, were brought to the Florida Bay Interagency Science Center, Key Largo, Florida. Small portions of the skin sample with evident microalgal accumulations were oxidized in boiling 30% nitric acid followed by addition of potassium dichromate. Cleaned diatoms were settled from the mixture for a minimum of 6 h and the remaining acid solution decanted. The settled diatoms were rinsed with deionized water. The rinsing/settling/decanting process was repeated six times until the solution reached a neutral pH.

For light microscopy (LM), cleaned diatoms were air-dried on cleaned No. 1 coverslips which were then mounted onto glass slides using Naphrax® (The Biology Shop, New South Wales, Australia). LM analyses were made using differential interference contrast (DIC) and an oil immersion planapochromatic lens (NA = 1.40) on a Nikon E600 microscope (×600 and ×1200 magnification) equipped with a Leica DFC425 digital camera. Diatom morphometrics were determined using Leica Application Suite version 3.7 imaging software. The relative abundances of individual taxa were determined by identifying and counting 502 diatom valves along arbitrary linear transects.

For scanning electron microscopy (SEM), subsamples of the cleaned material were dried onto aluminum stubs and sputter-coated with gold/palladium. SEM analyses were made with a JEOL-5900LV scanning electron microscope operated at 10–30 kV. Diatom terminology followed Round *et al.* (1990) and Denys (1997).

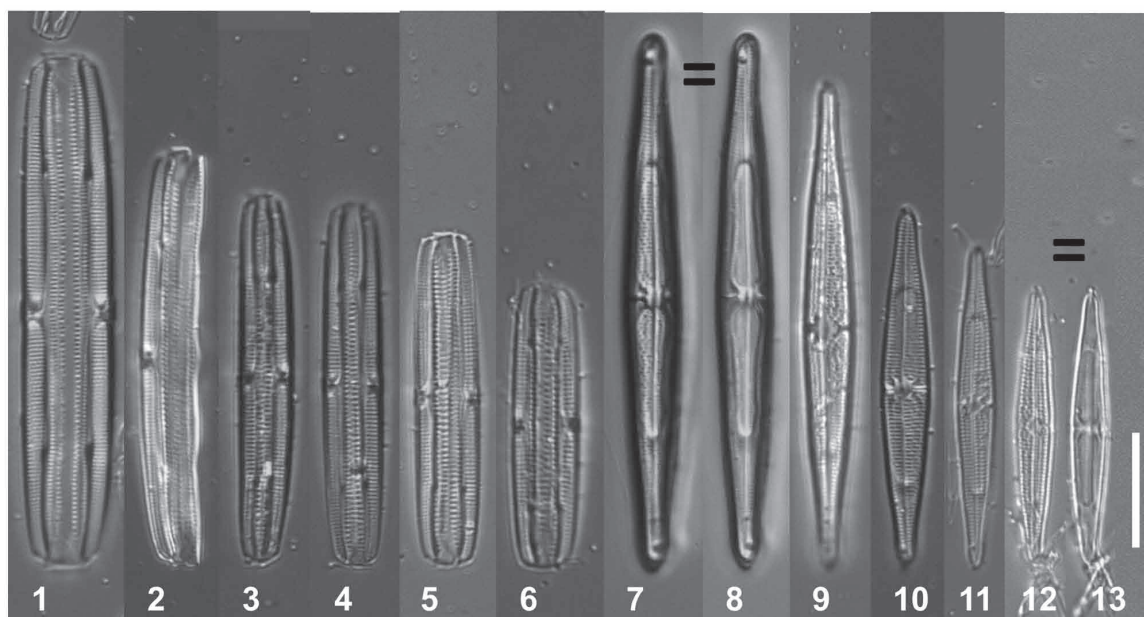
## Results

*Tursiocola* Holmes, Nagasawa & Takano (1993a: 5)

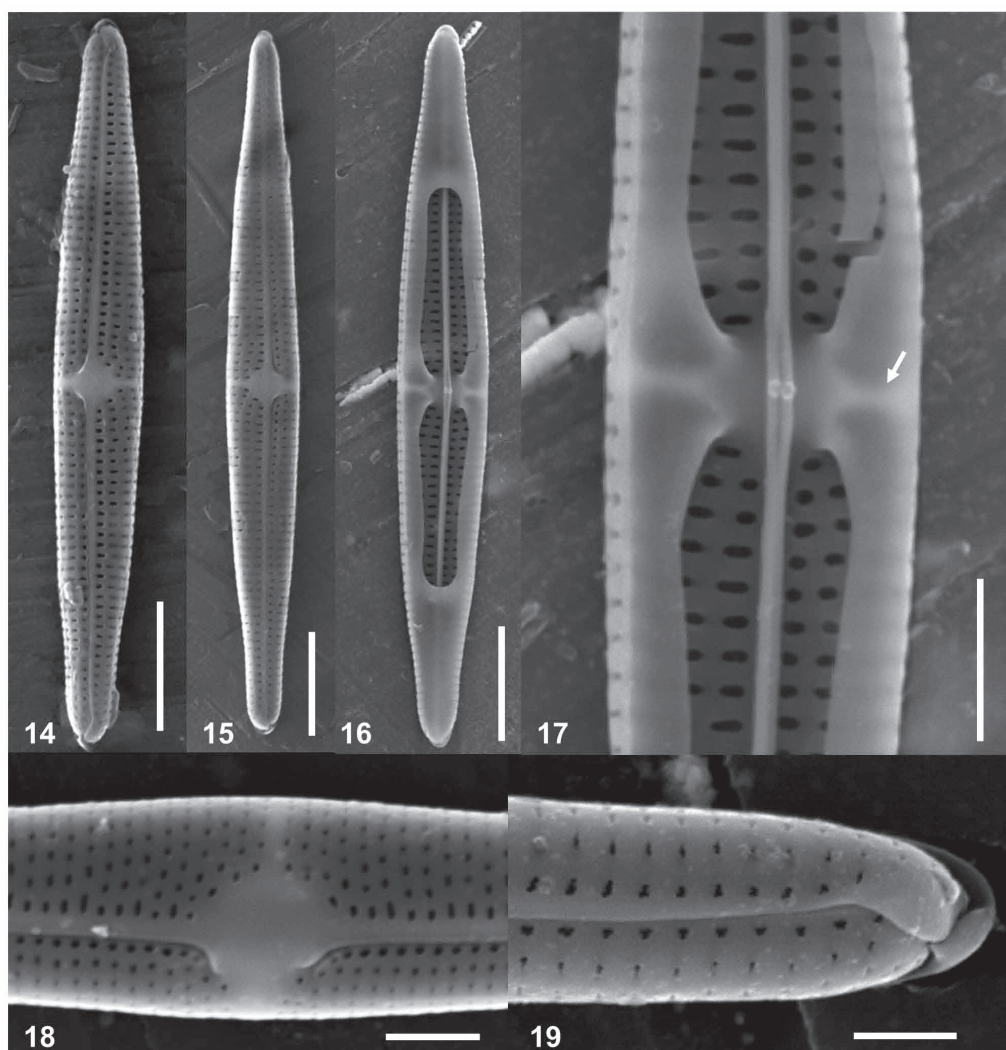
### *Tursiocola ziemanii* Frankovich & M.J. Sullivan, *sp. nov.* (Figs. 1–24)

The frustules are rectangular in girdle view with bluntly rounded ends and porose girdle copulae (Figs. 1–6). The valves are isopolar and narrowly lanceolate, tapering gradually from the middle of the valves to the juncture of the pseudosepta and the valve margin (approx. 1/4 of the valve length) and then tapering more rapidly towards rounded, produced, rostrate apices (Figs. 7–13). Length 20–61 µm, width 2.4–5.2 µm, length to width ratio 7.3–11.8. The valve face is slightly asymmetric around the narrow axial area with one half of the valve face wider than the other (Figs. 7, 9–12). The raphe is very fine and indistinguishable from the straight and more strongly silicified axial rib. The axial area is very narrow and widens at the diamond-shaped central area (Figs. 7, 9–12). The central area is intersected by a narrowing stauros that appears as a narrow highly refractive bar and extends to the valve margins where its width becomes only slightly larger than the interstriae width (Figs. 1–6). The transapical striae are slightly convergent/disrupted around the central area becoming mostly parallel towards the apices (Fig. 10), 22–25 in 10 µm. By focusing through the valve, pseudosepta can be seen to extend over approximately 1/4 of the valve length from the apices which then continue as narrow strips along the valve margin, widening in the central area where they fuse with the stauros forming a butterfly-like structure and two pyriform-shaped voids on either side of the central area (Figs. 8, 13).

**Type:**—UNITED STATES. Florida: Florida Bay, skin samples removed from a recently dead individual of a West Indian manatee *Trichechus manatus* in the vicinity of Coon Key, 25° 03' 18" N, 80° 44' 10" W, T.A. Frankovich, 28 October 2013 (holotype CAS! 223047, Figs. 1–24; isotypes ANSP! GC59139, BM! 101 786, BRM! Zu10/6).



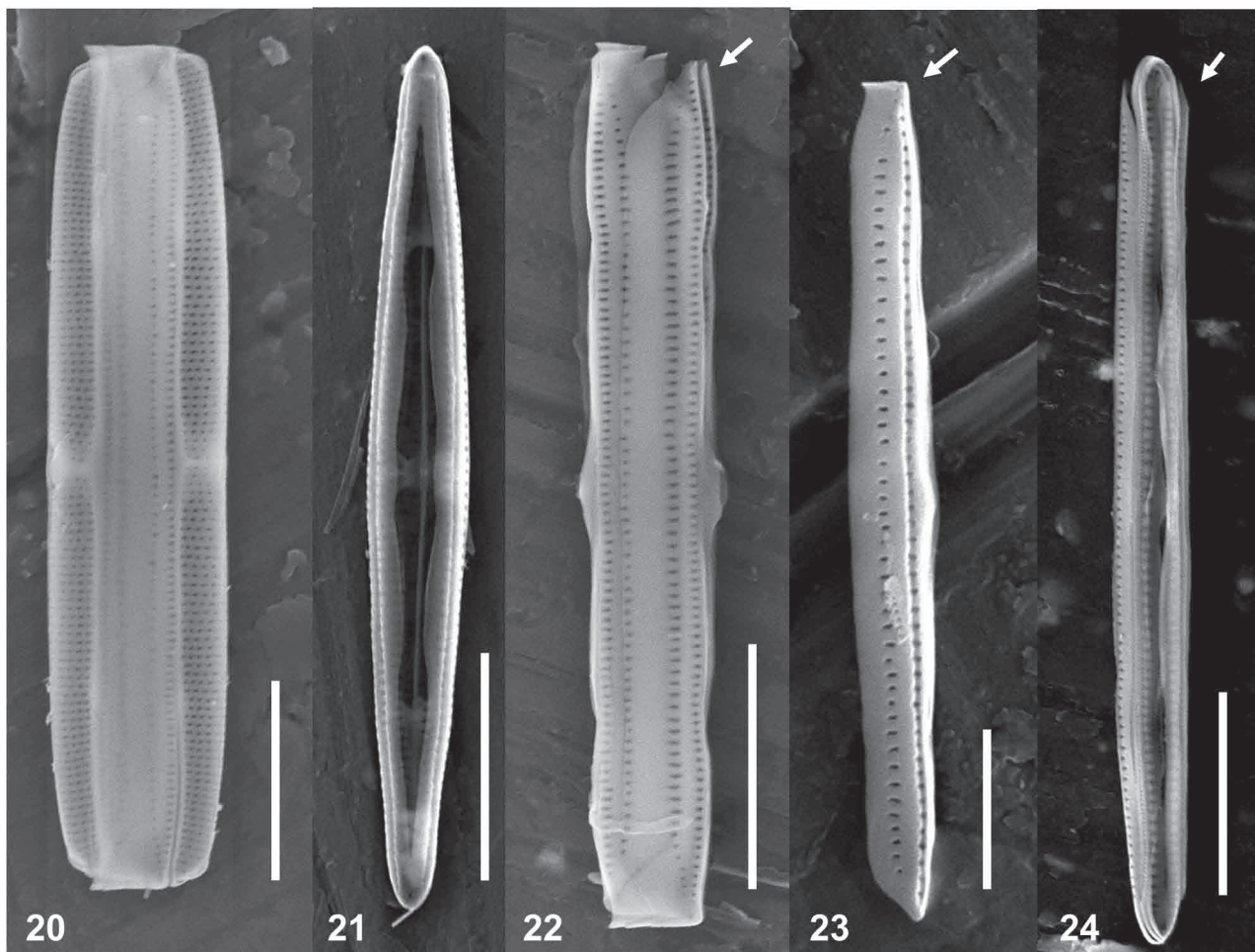
**FIGURES 1–13.** *Tursiocola ziemanii*. Type population, LM. 1–6. Frustules in girdle view showing size range and morphological variation. 7–13. Specimens in valve view showing size range. Scale bars: 1–13 = 10 µm. = indicates same specimen at different foci.



**FIGURES 14–19.** *Tursiocola ziemanii*. Type population, SEM. 14–15. External views of whole valves showing axial and central areas. 16. Internal view of whole valve showing pseudosepta and butterfly structure. 17. Detail of butterfly structure and internal central area with stauros (arrow) and two knobs on the raphe rib. 18. Detail of external central area showing diamond-shaped central area, stauros and deflected proximal raphe ends. 19. Detail of external valve apex showing apparently bifurcated distal raphe ends. Scale bars: 14–16 = 5 µm; 17–18 = 2 µm; 19 = 1 µm.



**SEM morphology:**—Externally, the valve mantle slopes steeply without any clear transition between the valve face and mantle (Figs. 14–15, 18–20). The valve face has uniseriate transapical striae composed of oval areolae extending onto the entire valve mantle (Figs. 14–15, 18–20). The mantle margin is narrow and slightly more silicified than the interstriae area (Fig. 20). The areolae are arranged in fairly straight longitudinal rows, approximately 23 areolae in 10  $\mu$ m (Figs. 14–15, 19). A straight, narrow, and more strongly silicified axial rib lies within the axial area that widens very slightly towards the central area (Figs. 14–15, 18). The raphe is very fine, straight and slightly eccentric (Figs. 14–15, 18). The central area is diamond-shaped with a narrow unpunctate stauros that extends to the valve margins (Figs. 14–15, 18). The stauros is slightly wider on the primary side of the valve (Figs. 14–15, 18). The external proximal raphe ends are simple, deflected towards the secondary side of the valve, and lie along the edge of the central area terminating where the stauros extends towards the valve margin (Fig. 18). The distal raphe ends are apparently bifurcated and obscured by overhanging siliceous flaps that bend towards the same side of the valve at both apices (Fig. 19). A siliceous rim curves around the valve apex (Fig. 19). A flange-shaped siliceous outgrowth is sometimes observed extending from the mantle on one side of the apex at one of the poles (Fig. 14).



**FIGURES 20–24.** *Tursiocola ziemanii*. Type population, SEM. 20. Entire frustule in girdle view showing cingulum with 2 copulae, each with a double row of pores. 21. Internal view of valve with attached copula. 22. Cingulum comprised of 2 copulae open on one end (arrow) with 2 rows of pores. 23. Isolated copula showing closed end (arrow) and two rows of pores. 24. Internal view of cingulum showing open (arrow) and closed ends of copulae. Scale bars: 20–22, 24 = 10  $\mu$ m; 23 = 5  $\mu$ m.

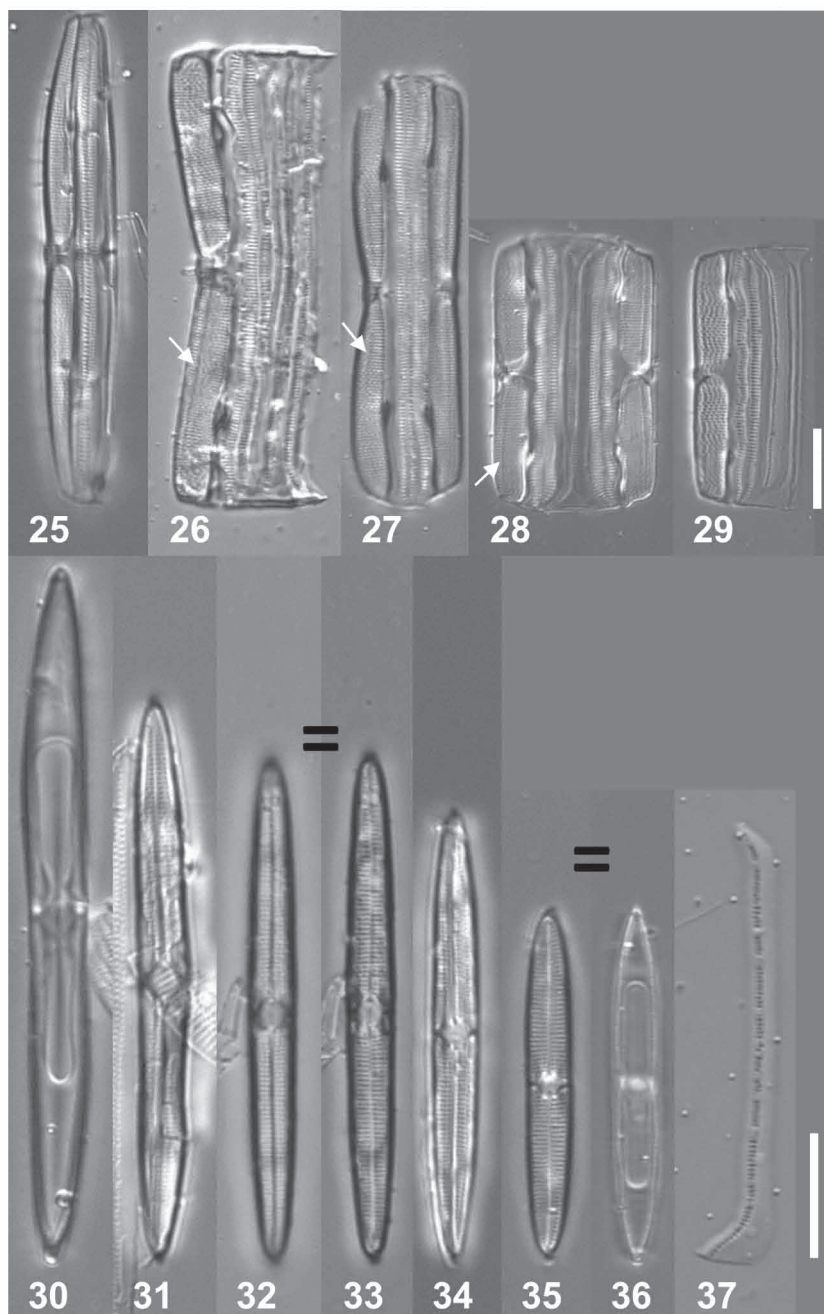
Internal views of the valves reveal the butterfly-like structure that connects the pseudosepta to the central area and stauros (Figs. 16–17, 21). The pseudosepta extend from the apices as siliceous plates for approximately one-quarter of the valve length and then continue as narrow strips that run along the valve margins before widening at the “wings” of the butterfly-like structure in the central area (Fig. 16). The narrow strips of the pseudosepta briefly widen towards the valve center forming broad concave “wings” of the butterfly structure (Figs. 18–19). The pseudosepta and the butterfly-like structure enclose two pyriform-shaped areas on either side of the central area (Figs. 16–17). Internally, the raphe slits open along the middle of a strong siliceous rib that widens slightly in the central area (Figs. 16–17). Two knob-like structures are present on the rib on opposing sides of the raphe at the valve center (Fig. 17). The internal

central area is hexagonal and fuses with the broad wings of the butterfly-like structure at an abrupt near 90° angle (Fig. 17). A narrow stauros intersects the central area (Fig. 17).

The girdle is composed of two copulae that are open on one end (Figs. 20–24) with a double row of transapically elongated pores, 17–22 in 10 µm (Figs. 20, 22–23). In whole frustules, the advalvar row is partially obscured by the valve mantle (Fig. 20).

**Etymology:**—the epithet honours Dr. Joseph C. Zieman (1943–), in recognition of his generous support of diatom research in Florida Bay.

***Tursiocola varicopulifera* Frankovich & M.J. Sullivan, *sp. nov.* (Figs. 25–46)**

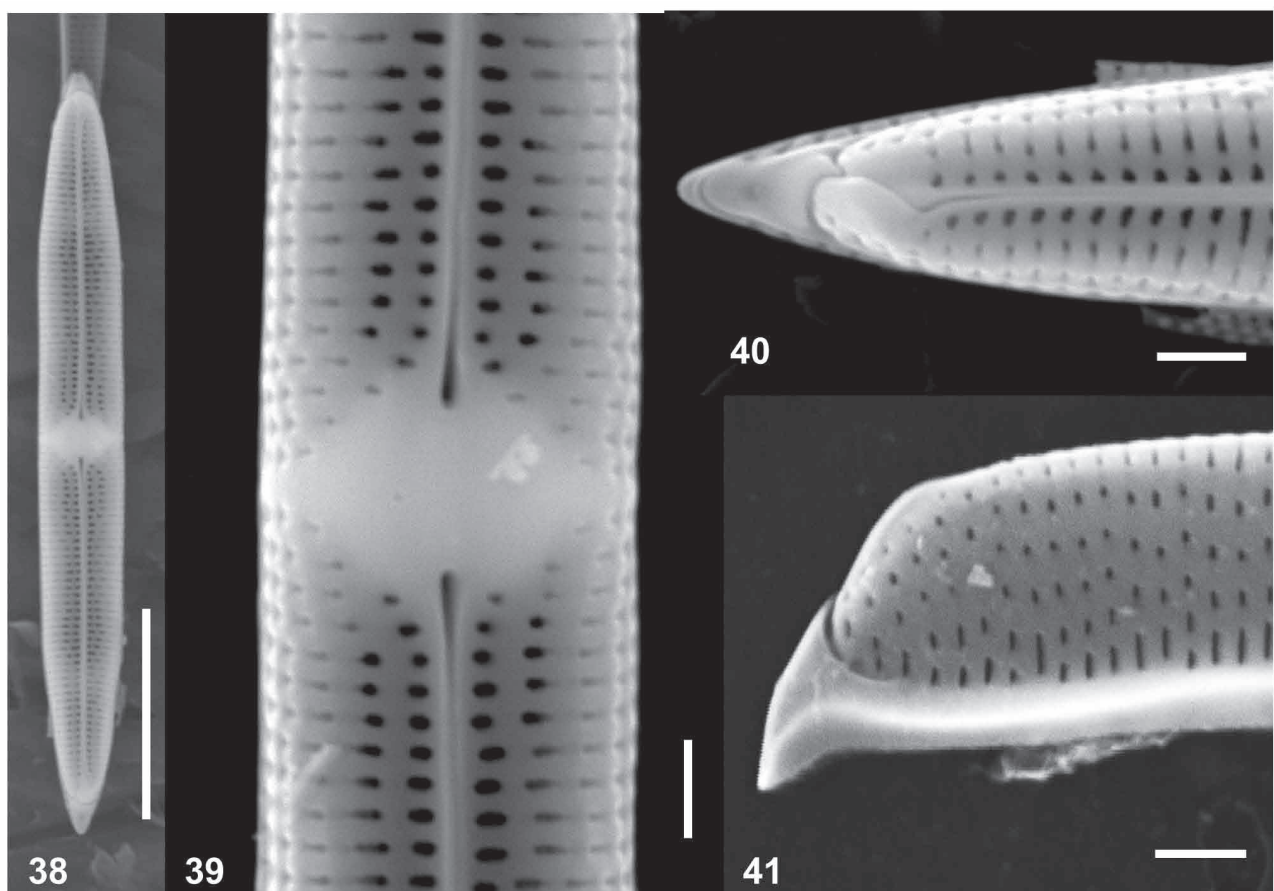


**FIGURES 25–37.** *Tursiocola varicopulifera*. Type population, LM. 25–29. Frustules in girdle view showing size range and morphological variation. Arrows indicate shadow lines of internal raphe ribs. 30–36. Specimens in valve view showing size range. 37. Isolated abvalvar copula with 1 row of pores. Scale bars: 25–37 = 10 µm. = indicates same specimen at different foci.

The frustules are narrow, broadly rectangular to constricted in the middle in girdle view with bluntly rounded ends and striated girdle bands that extend slightly beyond the valve apices (Figs. 25–29). The valves are isopolar and linear lanceolate (Figs. 30–32, 34–35) with

wide mantles (Figs. 25–29), and sub-acute apices (Figs. 30–36). Length 31–57  $\mu\text{m}$ , width 2.9–4.7  $\mu\text{m}$ , length to width ratio 10.3–12.3. The raphe is straight and lies within a narrow axial area (Figs. 30–32, 34–35). The proximal raphe ends are straight, expanded, pore-like, and terminate within a large, circular central area (Figs. 30–32, 34–35). The central area is intersected by a narrow rectangular stauros (Figs. 30–32, 34–35) that extends down the mantle and connects with a broad hyaline area along the margin of the middle of the valves (Figs. 25–29). Also visible in girdle view when focused on the plane of the raphe is a refractive line extending from the apices to the edge of the central area (Figs. 26–29). This refractive line is likely evidence of an internal siliceous rib associated with the raphe. The transapical striae are slightly convergent in the middle of the valve becoming parallel towards the apices (Figs. 32–35), 25–28 in 10  $\mu\text{m}$ . The transapical striae are shortened in the middle of the valve where they terminate before reaching the valve margin (Figs. 25–29). By focusing through the valve, pseudosepta can be seen to extend over approximately 1/5 of the valve length from each apex (Figs. 30–36) and then continue as narrow strips along the valve margin before connecting with the butterfly-like structure (Figs. 30–36). The pseudosepta and the butterfly-like structure enclose two oblong-shaped areas with slight constrictions in their middle on either side of the central area (Figs. 30, 36). The girdle is composed of two to four copulae of two different types (Figs. 25–29, 37). The advalvar copulae (*i.e.*, valvocopulae), present in all frustules, are more coarsely striated and have two undulating rows of linear pores (Figs. 25–29). When present, abvalvar bands have relatively finer striations consisting of a single row of smaller linear pores (Figs. 26, 28–29, 37). The row of pores on the abvalvar copulae curve toward the advalvar copulae (Figs. 26, 28–29, 37).

**Type:**—UNITED STATES. Florida: Florida Bay, skin samples removed from a recently dead individual of a West Indian manatee *Trichechus manatus* in the vicinity of Coon Key, 25° 03' 18" N, 80° 44' 10" W, T.A. Frankovich, 28 October 2013 (holotype CAS! 223046, Figs. 25–56; isotypes ANSP! GC59140, BM! 101 787, BRM! Zu10/7).

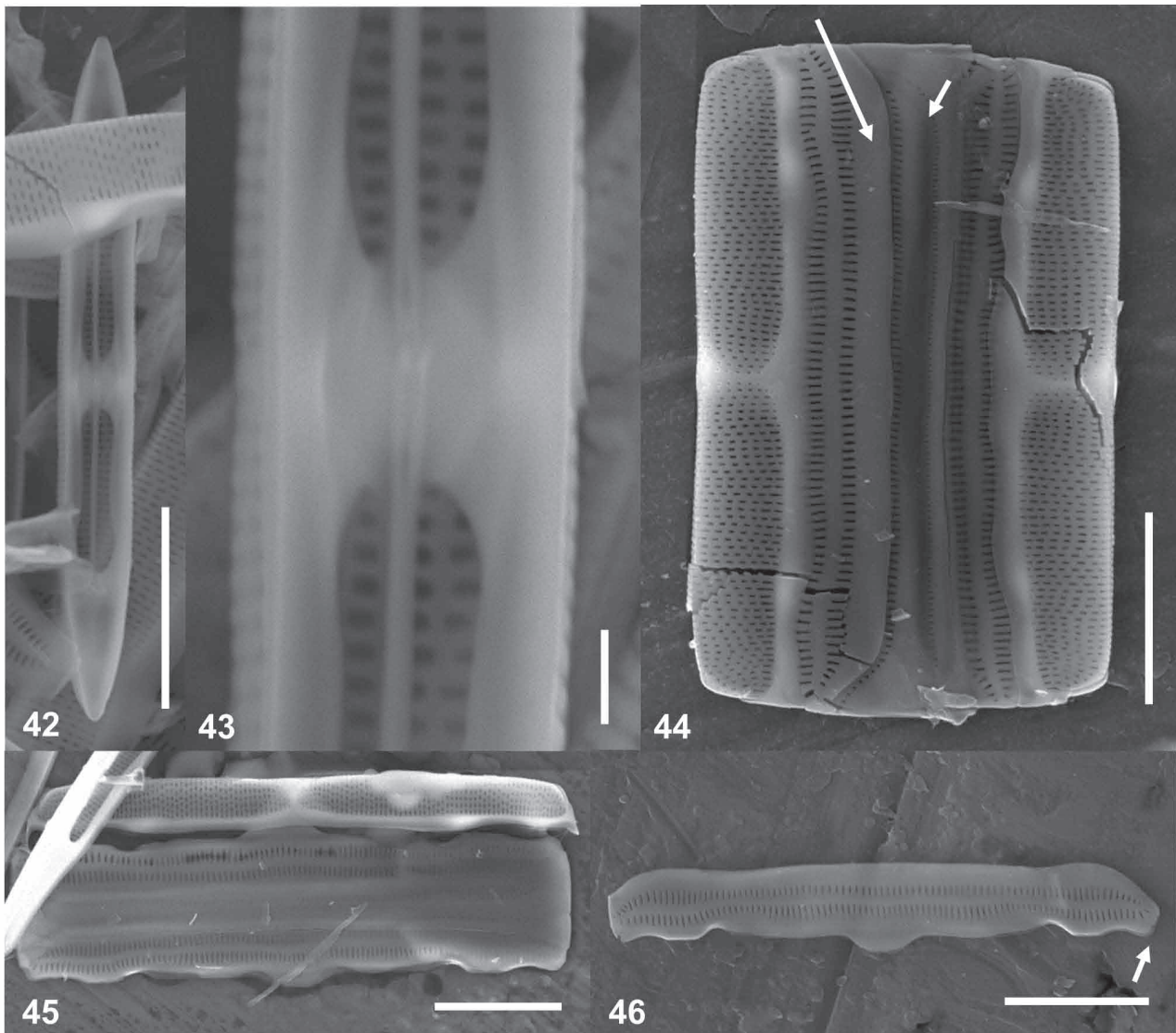


**FIGURES 38–41.** *Tursiocola varicopulifera*. Type population, SEM. 38. External view of whole valve showing axial and central areas. 39. Detail of external central area showing diamond-shaped central area, stauros and straight expanded proximal raphe ends. 40. Detail of external valve apex showing apparently bifurcated distal raphe ends. 41. Detail of external valve apex in mantle view showing transapically elongated areolae and spur-like extension of valve margin at apex. Scale bars. 38 = 10  $\mu\text{m}$ ; 39–41 = 1  $\mu\text{m}$ .

**SEM morphology:**—Externally, the valve face has uniseriate transapical striae composed of fine slit-like transapically elongated areolae of varying length (Figs. 38–41). The areolae are arranged in wavy longitudinal rows, approximately



17 areolae in 10  $\mu\text{m}$  along the transapical axis (Figs. 38–41, 44). The valve mantle is wide and slopes steeply without any clear transition between the valve face and mantle (Figs. 39–41, 44–45). The mantle margin is wide, heavily silicified, undulate, and expanded at the apices into spur-like extensions that expand outward from the apices and abvalvarly towards the copulae (Figs. 41, 44–45). The straight raphe lies within a narrow axial area (Figs. 38–40). The central area is large, diamond-shaped, and intersected by a narrow rectangular stauros that extends to the valve margins (Figs. 38–39, 44–45). The proximal raphe ends are straight, expanded, pore-like, and terminate slightly within the hyaline central area but before the rectangular stauros (Figs. 38–39). The distal raphe ends are apparently bifurcated and obscured by overhanging siliceous flaps that bend towards the same side of the valve at both apices (Fig. 40).



**FIGURES 42–46.** *Tursiocola varicopulifera*. Type population, SEM. 42. Internal view of whole valve showing pseudosepta and butterfly structure. 43. Detail of butterfly structure and internal oval central area with two knobs on the raphe rib. 44. Entire frustule in girdle view showing differentiated copulae and wide mantle areas. Long arrow indicates valvocopula; short arrow indicates abvalvar copula. 45. Valve and cingulum showing connections between valvocopula and valve margin. 46. Isolated valvocopula showing 3 tabs on advalvar side and 2 rows of elongated pores. Arrow indicates open end of valvocopula. Scale bars: 42, 44, 46 = 10  $\mu\text{m}$ ; 43 = 1  $\mu\text{m}$ ; 45 = 5  $\mu\text{m}$ .

Internally, the pseudosepta extend from the apices as siliceous plates for approximately one-fifth of the valve length, which then continue as narrow strips that run along the valve margins before widening into very broad concave “wings” of the butterfly-like structure in the central area (Fig. 42). The narrow strips of the pseudosepta briefly widen towards their middle (Fig. 42). The pseudosepta and the butterfly-like structure enclose two oblong-shaped voids on either side of the central area (Fig. 42). The oblong-shaped voids are constricted in the middle (Fig. 42). Internally, the raphe lies along the center of a strong siliceous rib (Figs. 42–43). Two knob-like structures are present on the rib on opposing sides of the raphe at the valve center (Fig. 43). The center of the butterfly-like structure is apically elongated

and oval (Fig. 43). The wings of the butterfly-like structure are very broad, concave, and connect gradually with the marginal strips of the pseudosepta (Fig. 43).

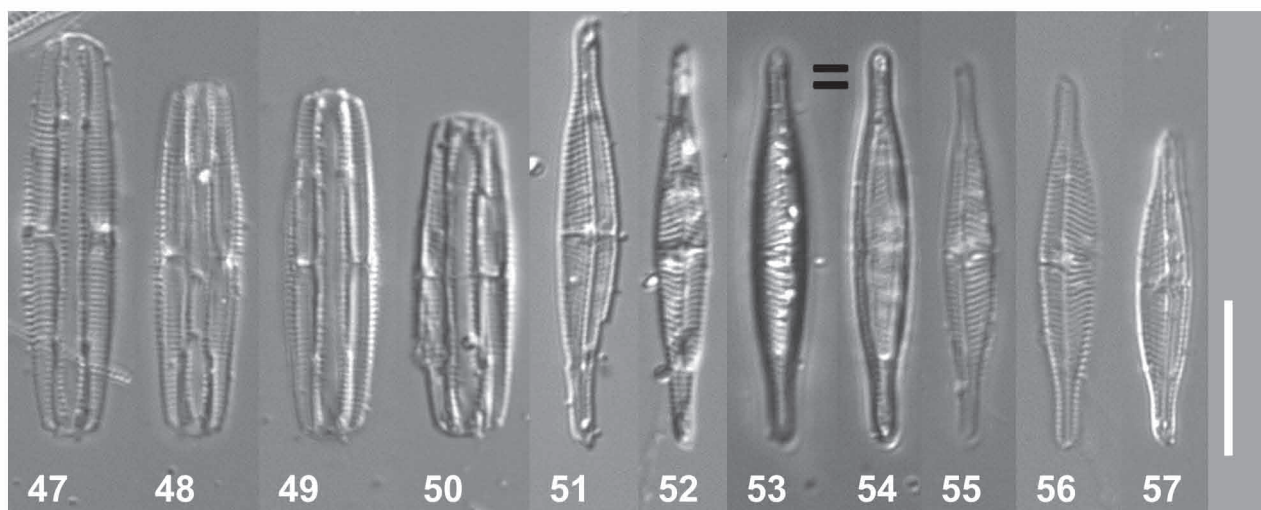
The copulae are differentiated into two types with wide advalvar copulae (*i.e.*, valvocopulae) possessing two rows of transapically elongated linear pores, 22–26 in 10  $\mu\text{m}$ , and thinner abvalvar copulae possessing a single row of finer transapically elongated pores, 27–32 in 10  $\mu\text{m}$ , (Figs. 44–45). The valvocopula is open on one end (arrow in Fig. 46) with three advalvar tabs on each side. These tabs underlie the valve mantle (Figs. 44–45). One tab is located in the middle and the other two are located before the open and closed ends of the copula (Fig. 46).

**Etymology:**—From Latin *varie* (differently), *copula* (connecting band) and *-fera* (bearing), with reference to the bearing of copulae of different types which are diagnostic for identification of this species in LM in girdle view.

***Tursiocola costata* Frankovich & M.J. Sullivan, *sp. nov.* (Figs. 47–66).**

The frustules are linear rectangular, slightly widened in the middle by elevated transapical interstriae costae, with bluntly rounded ends and two striated copulae (Figs. 47–50). The striae of the two copulae are located just below the valve margins and are separated by a relatively broad hyaline area (Figs. 47–50). The valves are slightly heteropolar and lanceolate with drawn out rostrate apices (Figs. 51–57). Length 17–29  $\mu\text{m}$ , width 2.5–3.9  $\mu\text{m}$ , length to width ratio 6.3–9.8. The heteropolarity of the valves is evidenced by small differences in the lengths of the valve halves or differences in the degree to which the apices are drawn out (*i.e.*, one valve end may be more rostrate than the opposing end). The valve face is also asymmetric around the narrow axial area with one half of the valve face wider than the other (Figs. 51–53, 55–57). The axial area bends towards the thinner valve half (Figs. 51–53, 55–57). The raphe is not evident in LM. The central area is diamond-shaped and is intersected by a narrowing stauros that extends to the valve margin (Figs. 51–53, 55–57). The transapical striae are convergent throughout the valve face (Figs. 51–53, 55–57), 22–29 in 10  $\mu\text{m}$ . By focusing through the valve, pseudosepta can be seen to extend over approximately 1/5 to 1/4 of the valve length from the apices, which then continue as narrow strips along the valve margin before connecting with the central area (Figs. 51–52, 54, 57).

**Type:**—UNITED STATES. Florida: Florida Bay, skin samples removed from a recently dead individual of a West Indian manatee *Trichechus manatus* in the vicinity of Coon Key, 25° 03' 18" N, 80° 44' 10" W, T.A. Frankovich, 28 October 2013 (holotype CAS! 223045, Figs. 47–68; isotypes ANSP! GC59141, BM! 101 788, BRM! Zu10/8).

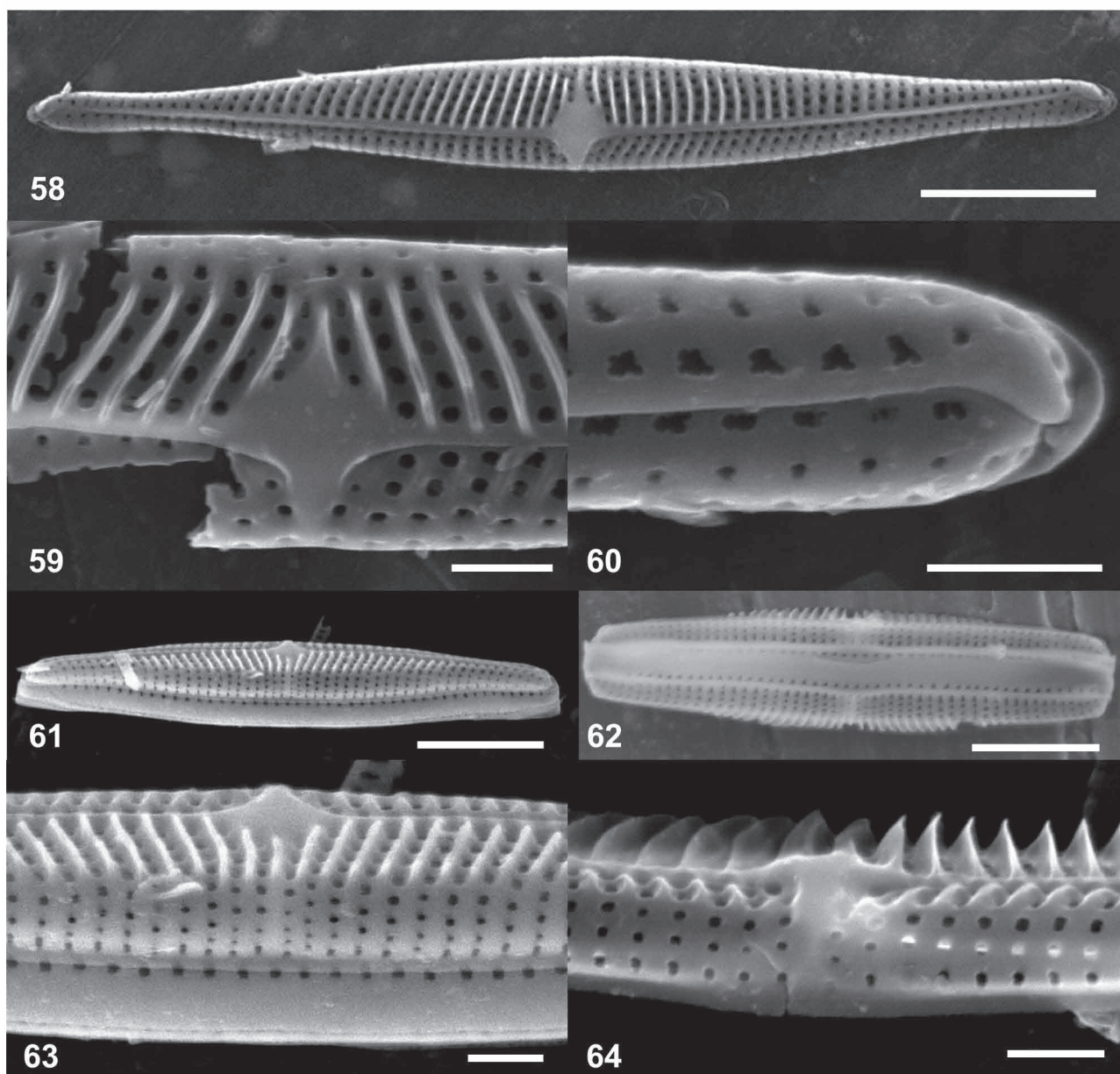


**FIGURES 47–57.** *Tursiocola costata*. Type population, LM. 47–50. Frustules in girdle view showing size range. 51–57. Specimens in valve view showing size range and morphological variation. Scale bars. 47–57 = 10  $\mu\text{m}$ . = indicates same specimen at different foci.

**SEM morphology:**—Externally, the valve face has convergent uniseriate transapical striae separated by raised interstriae for 1/2 to 2/3 of the valve length (Figs. 58, 61, 63–64). There is a clear transition between the valve face and the valve mantle (Figs. 61, 63–64). Interstriae costae are not present on the valve mantle where the transapical striae are parallel in the middle and slightly convergent towards the apices (Figs. 61, 63–64). The mantle edge is narrow with a clear transition between it and the upper mantle at the valve middle (Figs. 63–64). The raised interstriae costae are rounded on the narrower half of the valve face, and triangular with sharp edges in cross-section on the wider halves of the valve faces (Figs. 63–64). The transapical striae are composed of circular to oval to irregular areolae, approximately



18 areolae in 10  $\mu\text{m}$  along the transapical axis (Figs. 58, 60–64). A narrow strongly silicified rib lies within the axial area (Figs. 58, 60–61, 63–64). The raphe is very fine and lies immediately adjacent to the rib on the narrower half of the valve face (Fig. 58). The central area is raised (Figs. 61, 63–64), diamond-shaped and intersected by a narrow linear stauros about the width of the interstriae area (Figs. 58–59, 61, 63–64). A single interstriae costa is sometimes present in the stauros (Figs. 59, 63). The proximal raphe ends are expanded and deflected towards the narrower valve half (Fig. 59). The distal raphe ends are apparently bifurcated, obscured by overhanging siliceous flaps and deflected in the same direction as the proximal raphe ends (Fig. 60).



**FIGURES 58–64.** *Tursiocola costata*. Type population, SEM. 58. External view of entire valve showing drawn out rostrate apices, asymmetric valve face, bent axial area, diamond-shaped central area and narrow stauros. 59. External view of central area showing deflection of proximal raphe ends. 60. External view of apparently bifurcated distal raphe end. 61. External oblique view of entire valve with attached cingulum showing raised interstriae costae and convergent striae on valve face, raised central area, distinct valve mantle and 2 copulae, each with 1 row of pores. 62. Entire frustule in girdle view showing raised interstriae costae and cingulum with 2 copulae, each with a single row of pores adjacent to the valve margin. 63. Detail of valve center and cingulum in oblique view showing transitions between valve face, mantle and margin. 64. Detail of external valve center in oblique view showing raised interstriae costae, round areolae and narrow stauros. Scale bars: 58, 61–62 = 5  $\mu\text{m}$ ; 59–60, 63–64 = 1  $\mu\text{m}$ .

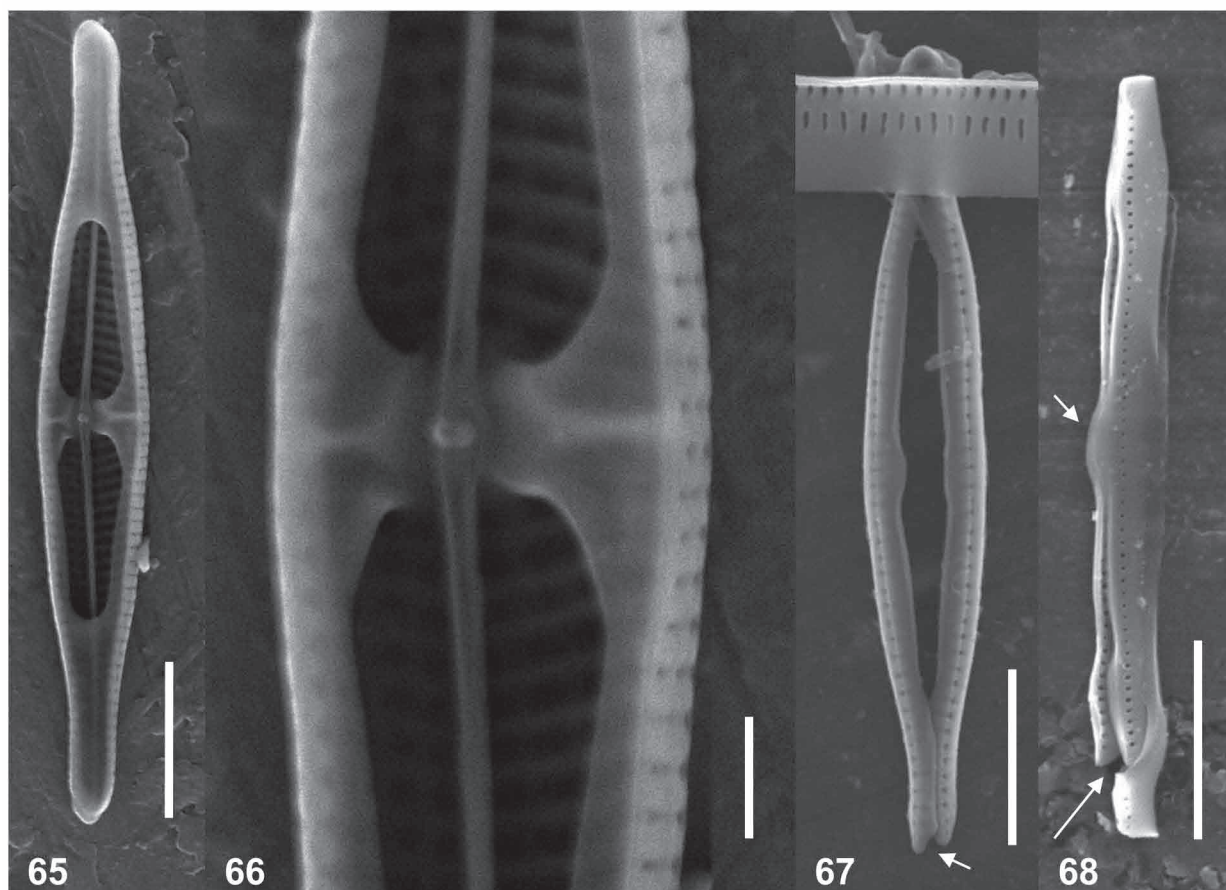
The interstriae transapical costae are also visible in the internal view of the valve (Figs. 65–66). The butterfly-like structure that connects the pseudosepta to the central area and the very narrow stauros is also clearly seen (Figs. 65–66). The pseudosepta extend from the apices as siliceous plates for approximately one-quarter of the valve length

(Fig. 65), which then continue as narrow strips that run along the valve margins before widening into broad concave “wings” of the butterfly-like structure in the central area (Figs. 65–66). The narrow strips of the pseudosepta briefly widen towards their middle (Fig. 65). The pseudosepta and the butterfly-like structure enclose two rounded pyriform-shaped voids on either side of the central area (Fig. 65). Internally, the raphe lies along the center of a strong siliceous rib that widens in the central area (Figs. 65–66). Two knob-like structures are present on the rib on opposing sides of the raphe at the valve center (Fig. 66). The center of the butterfly-like structure is hexagonal (Figs. 65–66) and connects with the wings of the butterfly-like structure at a near 90° angle (Fig. 66). A very narrow stauros intersects the central area (Fig. 66).

The girdle is composed of two copulae (Fig. 62), possessing a single row of circular to oval pores, 22–28 in 10 µm (Figs. 62, 67–68). The copulae are open on one end with tabs in the middle that extend advalvarly towards the valve margins (Figs. 67–68). In whole frustules, the pores are partially obscured by the valve mantle (Fig. 62).

**Etymology:**—From Latin *costa* (rib), with reference to the transapical interstriae costae which are diagnostic for identification of this species in SEM in valve and girdle views.

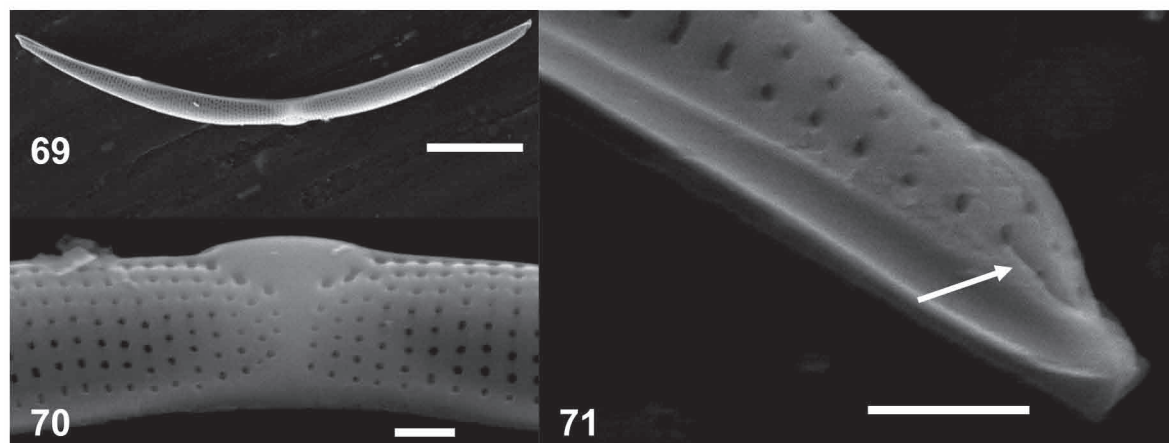
**Taxa relative abundances:**—Eighteen taxa from 11 genera were observed in a count of 502 valves from the type slide CAS 223045 (Table 1). The 3 newly described *Tursiocola* species comprised 89% of the valves counted. The relative abundances of *T. ziemanii*, *T. varicopulifera*, and *T. costata* were 52, 24, and 12%, respectively. None of the other described *Tursiocola* or *Epiphallaina* taxa were observed in the material, though two isolated valves of an unidentified *Tursiocola* taxon with strongly dorso-ventrally curved valves were observed in LM and SEM (Figs. 69–71). The scarcity of those specimens in the sample did not permit a comprehensive description at this time, but a butterfly-shaped shadow of thickened silica around the stauros (Figs. 69–70) suggests a *Tursiocola* species. The 14 other taxa observed in the valve count constituted only 11% of the valves counted.



**FIGURES 65–68.** *Tursiocola costata*. Type population, SEM. 65. Internal view of whole valve showing pseudosepta and butterfly structure. 66. Detail of butterfly structure and internal hexagonal central area with two knobs on the raphe rib. 67. Isolated copula showing internal structure and opening at one end (arrow). 68. Isolated copula in girdle view showing opening at one end (short arrow), a single row of pores, and a central tab (long arrow) on the advalvar side. Scale bars: 65, 67–68 = 5 µm; 66 = 1 µm.

**TABLE 1.** Relative abundances of diatom species observed in a count of 502 valves from the holotype slide of *Tursiocola costata*.

Taxon	Relative abundance (%)
<i>Tursiocola ziemanii</i> , sp. nov.	52.2
<i>Tursiocola varicopulifera</i> , sp. nov.	24.1
<i>Tursiocola costata</i> , sp. nov.	12.2
<i>Cocconeis</i> sp.	4.8
<i>Mastogloia lanceolata</i> Thwaites	1.0
<i>Cyclotella desikacharyii</i> Prasad	0.8
<i>Brachysira aponina</i> Kützing	0.8
<i>Nitzschia</i> cf. <i>liebetruthii</i> Rabenhorst	0.8
<i>Tabularia tabulata</i> (C. Agardh) Snoeijs	0.8
<i>Amphora</i> sp.	0.6
<i>Mastogloia crucicula</i> (Grunow) Cleve	0.4
<i>Amphora acutiuscula</i> Kützing	0.4
<i>Tursiocola</i> sp.	0.2
<i>Mastogloia ovalis</i> Schmidt	0.2
<i>Mastogloia</i> sp.	0.2
<i>Diploneis smithii</i> (Brébisson in W. Smith) Cleve	0.2
<i>Rhopalodia pacifica</i> Krammer	0.2
<i>Reimerothrix floridensis</i> Prasad	0.2



**FIGURES 69–71.** *Tursiocola* sp. SEM. 69. Entire valve showing acute apices and arcuate outline in mantle view. Fig. 70. Detail of external central area in mantle view showing raised central area, stauros and areolae. 71. Detail of external valve apex in side view showing thickened valve margin and distal raphe end curving around apex (arrow). Scale bars: 69 = 1 µm; 70–71 = 1 µm.

## Discussion

The three new species, *Tursiocola ziemanii*, *T. varicopulifera*, and *T. costata* are similar to other species in the epizoic genera *Tursiocola* and *Epiphallaina* in morphology with narrow linear to lanceolate valves, well-developed pseudosepta, stauros, internal raphe slits along the center of strong siliceous ribs, and uniseriate striae. They are also similar in that they live on the skin of aquatic mammals and other animals. *Tursiocola* is distinguished from *Epiphallaina* by the presence of the butterfly structure in the internal central areas of the valves of the former (Holmes *et al.* 1993a, Denys 1997). All 3 new species described here have distinct butterfly structures clearly placing them within the genus *Tursiocola*. It has been stated that *Epiphallaina* could be distinguished from *Tursiocola* in the structure of the copulae with *Epiphallaina* possessing copulae with a single row of pores and *Tursiocola* having two rows (Holmes *et al.* 1993a,



Denys 1997, Wetzel *et al.* 2012). The different number of rows of pores on the copulae of *T. ziemanii* (2 rows), *T. varicopulifera* (2 rows on valvocopulae, 1 row on abvalvar copulae) and *T. costata* (1 row) clearly make this distinction invalid.

*Tursiocola ziemanii*, *T. varicopulifera*, and *T. costata* exhibit several morphological characteristics that distinguish them from the other four described *Tursiocola* taxa (Table 2). *Tursiocola ziemanii* is most similar to *T. podocnemicola* and shares the following characteristics: simple external proximal raphe ends deflected towards the secondary side of the valve and apparently bifurcated external distal raphe ends deflected in the same direction as the proximal ends. *Tursiocola ziemanii* differs from *T. podocnemicola* in exhibiting a larger size range (20–61 versus 15–26 µm), less dense transapical striae (22–25 versus 30–35 in 10 µm), diamond-shaped versus rectangular central areas, narrow versus broad striae, and distinct versus indistinct butterfly structures, respectively (Table 2).

*Tursiocola varicopulifera* appears to be unique within the genus and differs from all other species in having a large, robust cingulum characterized by distinct valvocopulae that are differentiated from abvalvar copulae. All other *Tursiocola* species have undifferentiated copulae. The deep mantle with wide, strongly silicified valve margins, and the fine slit-like areolae of *T. varicopulifera* are also unique within the genus (Table 2). Shared morphological characteristics with the other *Tursiocola* species are few. The apparently bifurcated and deflected distal raphe ends of *T. varicopulifera* are shared characteristics with *T. ziemanii*, *T. costata*, and *T. podocnemicola*. The slightly convergent striae pattern in the valve middle which becomes parallel towards the apices is shared with *T. ziemanii*. Because of the deep mantle and the tendency for the cingulum to remain attached during sample cleaning, frustules and valves most often lie in girdle view making them easily recognizable on a prepared slide.

*Tursiocola costata* is also easily recognized and differentiated from all other species in the genus by the raised convergent interstriae costae on the valve face, visible in both valve and girdle views, and the heteropolar lanceolate valves with drawn out rostrate apices. *Tursiocola costata* is most similar to *T. ziemanii* with both species having a diamond-shaped external central area, deflected external proximal raphe ends, and a similar butterfly structure (Table 2).

Differences in the appearance of the butterfly structure are evident among *Tursiocola* species, and these may be useful in judging the relatedness among the species. Holmes *et al.* (1993a) described “an unpunctate membrane, originating at the valve margins which dips downward and fuses with a thickened central nodule, creating an open ended roofed chamber adjacent to each valve margin in the central area”, and used this feature in their description of the genus *Tursiocola*. Denys (1997) coined the term “butterfly structure” for this feature and further described the structure as originating from extensions of the pseudosepta. The length, width, and shape of these extensions differ among the *Tursiocola* species and vary from short and narrow with rapidly widening, concave borders in *T. olympica* (fig. 82 in Denys 1997) to wide and broad with gradually widening concave borders in *T. varicopulifera* (Fig. 43) to very short and wide with rectangular borders in *T. podocnemicola* (fig. 26 in Wetzel *et al.* 2012). These differences in the butterfly structure can be thought of as differences in the shape of the “wings”. The shapes of the butterfly structures of *T. ziemanii* and *T. costata* are very similar with broad concave wings that fuse with hexagonal central areas at abrupt near 90° angles (Figs. 17, 66) suggesting a closer relationship between the taxa than might be hypothesized by a comparison of other morphological characteristics. The absence or presence of the butterfly structure in *Epiphallina* and *Tursiocola*, respectively, is currently only one of two characteristics separating the genera given that differences in the structure of the cingulum are no longer valid, as exemplified by the single row of pores in copulae of *T. varicopulifera* and *T. costata*. The other distinguishing characteristic for separation of the genera is the arrangement of perforations on the hymenes (Holmes *et al.* 1989, 1993a, 1993b); however, this feature was not observable in the present study. Denys (1997) stated that support for the continued separation of *Epiphallina* from *Tursiocola* will depend on whether or not intergradations between the two are found. The seemingly reduced butterfly structure in *T. podocnemicola* may possibly represent an intergradation between the two genera. However, we argue for the continued separation of the genera based on the simple presence or absence of the butterfly structure.

Denys (1997) suggested that *Epiphallina* and *Tursiocola* are close to the Rhoicospheniaceae, but the lack of flexed and strongly heteropolar valves in these two genera did not permit a definitive placement within the family. The observations of flexed valves in the undescribed *Tursiocola* sp. (Fig. 70) and some specimens of *T. varicopulifera* (Fig. 26) and the heteropolar valves of *T. costata* may possibly provide a stronger argument for the inclusion of *Tursiocola* within the family Rhoicospheniaceae.

The very low species richness of the diatom assemblage observed on the skin of the manatee and the abundance of the newly described *Tursiocola ziemanii*, *T. varicopulifera* and *T. costata* suggests a unique environment for the development of these taxa. The salinity range experienced by these epizoic taxa is assumed to be large, reflecting the migratory habits of their West Indian manatee host from freshwater to marine environments. The sampled dead

**TABLE 2.** Comparison of morphological characteristics among *Tursiocola* species.

	<i>Tursiocola ziemanii</i>	<i>Tursiocola varicopulifera</i>	<i>Tursiocola costata</i>	<i>Tursiocola podocnemicola</i>	<i>Tursiocola staurolineata</i>	<i>Tursiocola omurai</i>	<i>Tursiocola olympica</i>
Length (µm)	20–61	31–57	17–29	15–26	15–35	20–35	14–22
Width (µm)	2.4–5.2	2.9–4.7	2.5–3.9	1.5–2.0	1.5–4	4–5	1.6–2.4
Length: width ratio	7.3–11.8	10.3–12.3	6.3–9.8	7.3–10.3	6.5–12.2	n.d.	7.1–11.7
Striae in 10 µm	22–25	25–28	22–29	30–35	28–36	30–32	35–38
Striae pattern	Slightly convergent/ disrupted in middle, becoming parallel towards apices	Slightly convergent in middle, becoming parallel towards apices	Convergent, with distinctively raised interstriae costae	Almost parallel	Parallel in middle, becoming slightly radial, finally convergent at apices	Parallel	Parallel in middle, becoming slightly radial, finally convergent at apices
Areolae	Oval	Fine, slit-like, transapically elongated	Circular to oval	Circular to transapically oval	Circular	n.d.	Circular
Valve outline	Narrowly lanceolate with produced, rostrate apices	Linear-lanceolate with sub-acute to acute apices	Lanceolate with drawn out rostrate apices	Linear-lanceolate with a distinct median constriction and sub-acute apices	Linear to narrowly lanceolate with sub-acute apices	Linear with a distinct median constriction and rostrate apices	Linear to narrowly lanceolate with sub-acute apices
Symmetry	Isopolar	Isopolar	Heteropolar	Isopolar	Slightly heteropolar	Slightly heteropolar	Slightly heteropolar
External central area	Diamond-shaped	Large, diamond-shaped	Diamond-shaped	Large, rectangular	Small, round	Very small, round	Large, rectangular
Stauros	Narrow, wider on the secondary side of valve	Narrow, rectangular	Very narrow, linear	Broad and widening towards mantle	Narrow and narrowing towards mantle	Very narrow, linear	Very broad, rhombic
External proximal raphe ends	Simple and deflected towards secondary side of valve	Straight, expanded, pore-like	Expanded, deflected towards secondary side of valve	Simple and deflected towards secondary side of valve	Straight, slightly expanded	n.d.	Straight, expanded

.....continued on the next page

**TABLE 2.** Comparison of morphological characteristics among *Tursiocola* species.

**TABLE 2** (Continued)

	<i>Tursiocola ziemanii</i>	<i>Tursiocola varicopulifera</i>	<i>Tursiocola costata</i>	<i>Tursiocola podocnemicola</i>	<i>Tursiocola staurolineata</i>	<i>Tursiocola omurai</i>	<i>Tursiocola olympica</i>
External distal raphe ends	Apparently bifurcated and deflected towards secondary side of valve	Apparently bifurcated and deflected towards secondary side of valve	Apparently bifurcated and deflected towards secondary side of valve	Bifurcated and deflected towards secondary side of valve	Strongly hooked with angular bend toward secondary side	n.d.	Strongly hooked toward secondary side
Butterfly structure	Broad concave wings fuse with hexagonal central area at an abrupt near 90° angle	Very broad concave wings, large oval central area	Broad concave wings fuse with hexagonal central area at an abrupt near 90° angle	Indistinct, very short but wide wings with fairly straight margins, barely extend from pseudosepta before fusing with rectangular central area	Narrow concave wings, oval central area	Narrow, concave wings	Narrow concave wings, circular central area
Internal knobs	2	2	2	2	2	n.d.	1–2
Cingulum	2 copulae open on one end with 2 rows of transapically elongated pores	2 valvocopulae, open on one end with 2 rows of transapically elongated pores and 2 abvalvar copulae with 1 row of finer linear pores	2 copulae open on one end with 1 row of circular to oval pores	2–3 open copulae each with 1 row of large pores and 2 <sup>nd</sup> short row of smaller pores	2 closed copulae with 2 rows of aligned pores	Closed copulae with 2 rows of pores	Copulae with 2 rows of pores
Habitat	Marine	Marine	Marine	Freshwater	Marine	Marine	Marine
References	This study	This study	This study	Wetzel <i>et al.</i> (2012)	Denys (1997)	Nemoto (1956), Denys (1997)	Hustedt (1952), Holmes <i>et al.</i> (1993a), Denys (1997)



manatee was found in central Florida Bay where salinities range from 20–45 psu (Boyer *et al.* 1999). The dominance of these new species (almost 90% of the valve count) and the lack of any other ceticolous taxa or *T. podocnemicola* on the manatee raise the question of host specificity, but there are many marine animals that remain unsampled for diatoms. Bodily contact is likely required for the transfer of epidermal diatom taxa from one host to another (Holmes *et al.* 1993a); therefore, host populations would have to mix and interact closely to develop epizoic diatom communities of similar species composition. Such close interactions between the cetaceans, the freshwater turtle from which *T. podocnemicola* was described, and the West Indian manatee are unlikely at best. The West Indian manatee is one of four living species of the aquatic mammal order Sirenia. The West Indian manatee inhabits the coastal areas and rivers of the Caribbean Sea and the Gulf of Mexico and ranges from Georgia and Florida in the southeastern USA through Central America to the northeast coast of Brazil (Domning and Hayek 1986). The other three species of the order Sirenia are the dugong (*Dugong dugon*) of the Indo-Pacific coasts, the West African manatee (*Trichechus senegalensis*) of the West African coasts, and the Amazonian manatee (*Trichechus inunguis*) of the freshwaters of the Amazon Basin. There is not any overlap in the geographical distribution of the four manatee species; therefore, distinct epizoic communities are a possibility, but this hypothesis remains untested. The so-called “ceticolous” diatom taxa have now been found on whales, porpoises, manatees and a freshwater turtle raising many questions related to general ecological principles such as host specificity, endemism, and biogeographical distribution of species. The sampling of additional animal taxa for epizoic diatoms is needed to shed more light on these topics.

#### An artificial key to *Tursiocola* species

1. Copulae differentiated, valvocopulae distinct from abvalvar copulae ..... *Tursiocola varicopulifera*
- Copulae undifferentiated ..... 2.
2. Transapical costae present on external valve face ..... *Tursiocola costata*
- Transapical costae absent ..... 3.
3. Valve outline linear with a distinct median constriction and rostrate apices ..... *Tursiocola omurai*
- Valve outline otherwise ..... 4.
4. External central area diamond-shaped ..... *Tursiocola ziemanii*
- External central area otherwise ..... 5.
5. External proximal raphe ends deflected ..... *Tursiocola podocnemicola*
- External proximal raphe ends straight ..... 6.
6. Stauros very broad ..... *Tursiocola olympica*
- Stauros narrow and narrowing towards mantle ..... *Tursiocola staurolineata*

#### Acknowledgments

We thank the University of Florida Aquatic Animal Health Program for the funding of SEM time at Florida International University, the George Barley Scholars Program and Dr. Joseph C. Ziemann of the University of Virginia for the funding of LM instruments, Tom Beasley of the Florida Center for Analytical Electron Microscopy at Florida International University for assistance with SEM, Officer Brandon Moore for assistance with manatee sampling, Dr. Dave Rudnick for use of Everglades National Park facilities and boats, and Mariska Brady for assistance with taxonomy. We also thank two anonymous reviewers and Editor Saúl Blanco Lanza for their constructive comments and recommendations that greatly improved the manuscript. The samples were collected under FWC permit MA067116-2. This is contribution number 714 from the Southeast Environmental Research Center.

#### References

- Bennet, A.G. (1920) On the occurrence of diatoms on the skin of whales. *Proceedings of the Royal Society of London Series B* 91: 352–357.  
<http://dx.doi.org/10.1098/rspb.1920.0021>
- Boyer, J.N., Fourqurean, J.W. & Jones, R.D. (1999) Seasonal and long-term trends in the water quality of Florida Bay. *Estuaries* 22: 417–430.  
<http://dx.doi.org/10.2307/1353208>
- Denys, L. (1997) Morphology and taxonomy of epizoic diatoms (*Epiphialina* and *Tursiocola*) on a sperm whale (*Physeter macrocephalus*) stranded on the coast of Belgium. *Diatom Research* 12: 1–18.

<http://dx.doi.org/10.1080/0269249X.1997.9705398>

- Domning, D.P. & Hayek, L.C. (1986) Interspecific and intraspecific morphological variation in manatees (Sirenia: *Trichechus*). *Marine Mammal Science* 2: 87–144.  
<http://dx.doi.org/10.1111/j.1748-7692.1986.tb00034.x>
- Hart, T.J. (1935) On the diatoms of the skin film of whales and their possible bearing on problems of whales movements. *Discovery Reports* 10: 247–282.
- Holmes, R.W. (1985) The morphology of diatoms epizoic on cetaceans and their transfer from *Cocconeis* to two new genera, *Benettella* and *Epipellis*. *British Phycological Journal* 20: 43–57.  
<http://dx.doi.org/10.1080/00071618500650061>
- Holmes, R.W., Nagasawa, S. & Nemoto, T. (1989) Epidermal diatoms on the Dall's porpoise landed at Otsuchi, Iwate, Japan. *Otsuchi Marine Research Center Reports* 15: 15–20.
- Holmes, R.W., Nagasawa, S. & Takano, H. (1993a). The morphology and geographic distribution of epidermal diatoms of the Dall's porpoise (*Phocoenoides dalli* True) in the Northern Pacific Ocean. *Bulletin of the National Science Museum, Tokyo Series B* 19: 1–18.
- Holmes, R.W., Nagasawa, S. & Takano, H. (1993b) A re-examination of diatom samples obtained from cetaceans collected off South Africa. *Bulletin of the National Science Museum, Tokyo Series B* 19: 127–135.
- Hustedt, F. (1952) Diatomeen aus der Lebengemeinschaft des Buckelwals (*Megaptera nodosa* Bonn.). *Archiv für Hydrobiologie* 46: 286–298.
- Linnæus, C. (1758) *Systema naturæ per regna tria naturæ, secundum classes, ordines, genera, species, cum characteribus, differentiis, synonymis, locis. Tomus I. Editio decima, reformata*. Salvius, Stockholm, 824 pp.
- Nemoto, T. (1956) On the diatoms of the skin film of the whales in the Northern Pacific. *Scientific Reports of the Whales Research Institute, Tokyo* 11: 99–132.
- Nemoto, T., Best, P.B., Ishimaru, K. & Takano, H. (1980) Diatom films on whales in South African waters. *Scientific Reports of the Whales Research Institute, Tokyo* 32: 97–103.
- Round, F.E., Crawford, R.M. & Mann, D.G. (1990) *The diatoms. Biology and morphology of the genera*. Cambridge University Press, Cambridge, 747 pp.
- Stacy, N., De Wit, M., Boylan, S., Gulland, F. & Frankovich, T. (2014) Diatoms in cytologic specimens of aquatic animals – Part II, dermal, respiratory, and gastric samples. *Veterinary Clinical Pathology* 43: 473–474.  
<http://dx.doi.org/10.1111/vcp.12198>
- Tiffany, M.A. (2011) Epizoic and epiphytic diatoms. In: Seckbach, J. & Kociolek, J.P. (Eds.) *The Diatom World*. Springer, New York, pp. 197–209.  
[http://dx.doi.org/10.1007/978-94-007-1327-7\\_8](http://dx.doi.org/10.1007/978-94-007-1327-7_8)
- Wetzel, C.E., Van De Vijver, B. Cox, E.J., Bicudo, D. de C. & Ector, L. (2012) *Tursiocola podocnemicola* sp. nov., a new epizoic freshwater diatom species from the Rio Negro in the Brazilian Amazon Basin. *Diatom Research* 27: 1–8.  
<http://dx.doi.org/10.1080/0269249X.2011.642498>